Cell, Vol. 101, 249–258, April 28, 2000, Copyright ©2000 by Cell Press

Functional and Genomic Analyses Reveal an Essential Coordination between the Unfolded Protein Response and ER-Associated Degradation

Kevin J. Travers,[3,6] Christopher K. Patil,[1,2,6] Lisa Wodicka,[4,7] David J. Lockhart,[4,7] Jonathan S. Weissman,[3,5] and Peter Walter[1,2,5]
[1]Howard Hughes Medical Institute
[2]Departments of Biochemistry and Biophysics
[3]Departments of Cellular and Molecular Pharmacology
University of California, San Francisco
San Francisco, California 94143
[4]Affymetrix, Incorporated
3380 Central Expressway
Santa Clara, California 95051

Summary

The unfolded protein response (UPR) regulates gene expression in response to stress in the endoplasmic reticulum (ER). We determined the transcriptional scope of the UPR using DNA microarrays. Rather than regulating only ER-resident chaperones and phospholipid biosynthesis, as anticipated from earlier work, the UPR affects multiple ER and secretory pathway functions. Studies of UPR targets engaged in ER-associated protein degradation (ERAD) reveal an intimate coordination between these responses: efficient ERAD requires an intact UPR, and UPR induction increases ERAD capacity. Conversely, loss of ERAD leads to constitutive UPR induction. Finally, simultaneous loss of ERAD and the UPR greatly decreases cell viability. Thus, the UPR and ERAD are dynamic responses required for the coordinated disposal of misfolded proteins even in the absence of acute stress.

Introduction

Proteins entering the secretory pathway fold within the confines of the endoplasmic reticulum (ER). To support efficient folding, the ER maintains an environment enriched in chaperones, glycosylation enzymes, and oxidoreductases (for a review, see Ellgaard et al., 1999). Despite this optimized environment, an inevitable consequence of the large flux of proteins through the ER is that the folding process occasionally fails, resulting in the production of irrevocably misfolded proteins. Two distinct processes have been described that help eukaryotic cells cope with this problem: ER-associated degradation (ERAD) and the unfolded protein response (UPR).

The ERAD system eliminates misfolded proteins via degradation in the cytosol (reviewed by Bonifacino and Weissman, 1998). Misfolded ER proteins are retrotranslocated across the ER membrane into the cytosol, where ubiquitin-conjugating enzymes target them for proteasomal degradation (Ward et al., 1995; McCracken and Brodsky, 1996; Qu et al., 1996; Werner et al., 1996; Biederer et al., 1997). ERAD requires a number of dedicated ER-resident factors, including the proteins Der1p, Der3p/Hrd1p, and Hrd3p (Hampton et al., 1996; Knop et al., 1996; Bordallo et al., 1998). ERAD substrates pass through the translocon as they exit the ER en route to the proteasome; hence, several components of the translocon and cytosolic degradation machinery are shared by ERAD and other cellular processes (Hiller et al., 1996; Wiertz et al., 1996; Pilon et al., 1997; Plemper et al., 1997; Zhou and Schekman, 1999).

A second means of coping with unfolded ER proteins is the UPR (reviewed by Chapman et al., 1998). The accumulation of unfolded ER proteins activates the transmembrane kinase/nuclease Ire1p (Cox et al., 1993; Mori et al., 1993; Shamu and Walter, 1996), which initiates the nonconventional splicing of *HAC1* mRNA. This leads to production of Hac1p, a bZIP transcription factor (Cox and Walter, 1996; Mori et al., 1996; Sidrauski et al., 1996; Sidrauski and Walter, 1997), and ultimately transcriptional induction of UPR target genes. Regulation of gene expression by the UPR allows the cell to tolerate folding stress and presumably assists in correction of the insult that caused unfolded proteins to accumulate (Cox et al., 1993; Mori et al., 1993).

While the mechanism by which the UPR signal is transmitted from the ER to the nucleus is well characterized, it is less clear how this response corrects misfolding. Of the small number of UPR target genes identified thus far, most encode ER-resident chaperones, as might be expected for a response to the accumulation of unfolded proteins (Chapman et al., 1998). In addition, components of the phospholipid biosynthetic pathways are targets, suggesting a role for the UPR in maintenance and biogenesis of the ER membrane (Cox et al., 1997; Kagiwada et al., 1998). Identification of the complete set of UPR target genes thus promised to provide insight into the means by which the cell copes with folding stress and adjusts the capacity of protein folding in the ER according to need. Here, we have used genome-wide expression analysis in conjunction with specific mutations to identify genes whose expression is specifically induced by the UPR in the budding yeast *Saccharomyces cerevisiae.*

Results

Defining the Targets of the UPR

We identified transcriptional targets of the UPR by monitoring mRNA levels using high-density oligonucleotide arrays (Wodicka et al., 1997). We induced the UPR by treating cells with two chemical agents that disrupt protein folding in the ER: the strong reducing agent dithiothreitol (DTT), which prevents disulfide bond formation, and the drug tunicamycin, which inhibits N-linked glycosylation. Neither of these agents is known to affect protein folding outside the secretory pathway. Furthermore, because these agents interfere with ER folding by different mechanisms, any gene regulation resulting from

[5]To whom correspondence should be addressed (e-mail: jsw1@itsa.ucsf.edu [J. S. W.], walter@cgl.ucsf.edu [P. W.]).
[6]These authors contributed equally to this work.
[7]Present address: Genomics Institute of the Novartis Research Foundation (GNF), 3115 Merryfield Row, San Diego, California 92121.

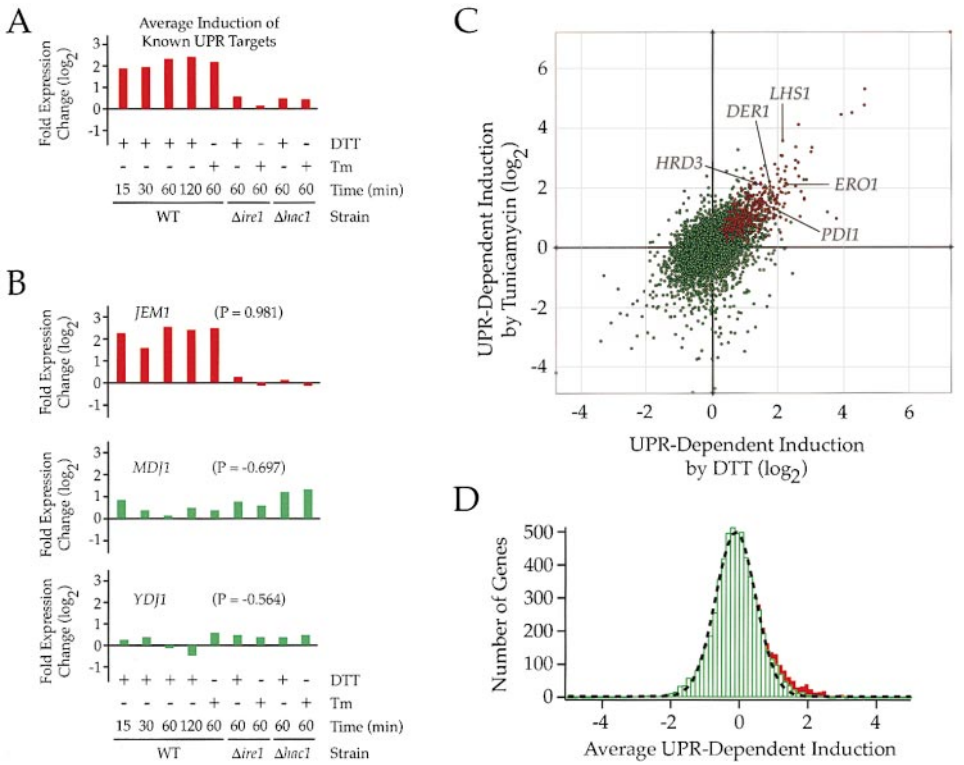

Figure 1. Identification of the Transcriptional Targets of the UPR

(A) Determination of the canonical UPR. For each of the indicated nine conditions (wild-type cells treated with DTT for 15, 30, 60, or 120 min; wild-type cells treated with tunicamycin (Tm) for 60 min; Δ*ire1* cells treated with DTT or Tm for 60 min; or Δ*hac1* cells treated with DTT or Tm for 60 min), the average of the $\log_2$ of fold induction for seven known UPR targets (*KAR2*, *LHS1*, *ERO1*, *PDI1*, *EUG1*, *FKB2*, and *INO1*) was calculated.

(B) Graphical representation of the expression pattern for three DnaJ homologs. Correlation coefficients (P) were calculated for each gene in the yeast genome, comparing its expression pattern in the nine conditions to that of the canonical profile. Represented here are three DnaJ homologs, with their respective correlation values. *JEM1* encodes an ER-resident protein, while *MDJ1* and *YDJ1* encode mitochondrial and cytosolic proteins, respectively.

(C) Comparison of UPR-dependent induction by DTT and tunicamycin. UPR-dependent induction was calculated by dividing the average of fold changes in wild-type cells by the average of fold changes in two UPR-deficient strains (see the Experimental Procedures). Points representing ORFs that satisfy the criteria for being targets of the UPR (i.e., P value $>$ 0.81, Z-test $>$ 3.6, and average induction in wild-type cells $>$ 1.5) are red, while points representing all other genes are green. For illustration, positions of three previously known targets of the UPR (*ERO1*, *PDI1*, and *LHS1*) are indicated, as well as two targets identified in this work (*DER1* and *HRD3*).

(D) Distribution of UPR induction. Shown is a histogram of the number of ORFs at a given distance along the diagonal of the scatter plot in (C), which we take as a combined measure of DTT and tunicamycin UPR-dependent induction. Green bars represent data from genes called as nontargets of the UPR, while red bars represent the contribution from the set of target genes. Shown with a dotted line is the Gaussian fit to the distribution of nontargets, which highlights the asymmetry of induction.

both treatments is likely to result from ER protein misfolding rather than nonspecific effects.

We prepared RNA samples for array hybridization from wild-type cells grown under five conditions: exposure to DTT for 15, 30, 60, or 120 min, or exposure to tunicamycin for 60 min. For each open reading frame (ORF), we determined the fold change in expression due to each drug treatment by comparing its expression level in the treated sample to its level in an untreated control. In order to eliminate from consideration ORFs with UPR-independent transcriptional changes, we also measured fold changes in strains bearing either a deletion of *IRE1* (Δ*ire1*) or *HAC1* (Δ*hac1*). These UPR-deficient strains are unable to transduce the UPR signal from the ER to the nucleus (Cox et al., 1993; Mori et al., 1993, 1996; Cox and Walter, 1996). We treated both mutant strains with either DTT or tunicamycin for 60 min and determined the fold change in expression by comparison to an untreated control. Thus, for each ORF, there are nine induction measurements: five from treatment of a wild-type strain and four from treatment of UPR-deficient strains.

We then defined a canonical response profile for a UPR target gene by combining the array expression data for seven previously reported UPR targets: *KAR2*, *EUG1*, *PDI1*, *LHS1*, *FKB2*, *ERO1*, and *INO1* (Chapman et al., 1998). For each of the nine treatment conditions, we defined the canonical response as the average of the fold changes in that condition for each of the known target genes. As anticipated, UPR targets showed strong induction in each of the wild-type conditions and little or no induction in the four UPR-deficient conditions (Figure 1A). The canonical profile shows that the UPR is rapid: induction of target genes was essentially complete after 15 min and was maintained over the time course of DTT treatment. Thus, the time course of DTT

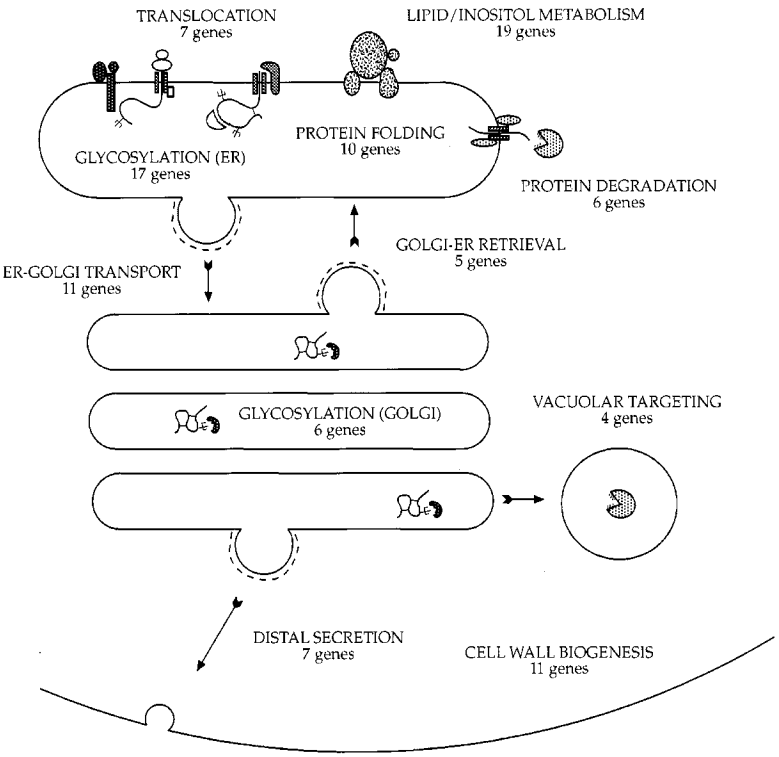

Figure 2. Many Aspects of Secretory Pathway Function Are Regulated by the UPR

A schematic diagram of the secretory pathway, with a classification of the genes identified as targets of the UPR. See Table 1 for details.

induction in effect provides four independent measurements of UPR activity under fully induced conditions. The magnitude of the response was comparable in DTT- and tunicamycin-treated cells.

We employed three criteria to identify novel targets of the UPR. First, we required targets of the UPR to exhibit expression patterns that matched those of known UPR targets. For each ORF, we calculated the correlation between the expression pattern of that ORF and the canonical profile. We selected ORFs as candidate targets if this correlation was no worse than that of *KAR2*, the previously identified UPR target with the lowest correlation to the canonical profile ($P = 0.81$). This analysis is illustrated in Figure 1B, in which the expression patterns for three DnaJ homologs are displayed along with their correlations to the canonical profile. The gene encoding the ER-resident chaperone Jem1p shows high correlation ($P = 0.98$), suggesting that *JEM1* is a target of the UPR. In contrast, genes encoding DnaJ homologs localized to the mitochondria (*MDJ1*) or the cytosol (*YDJ1)* show little correlation ($P = -0.70$ and -0.56, respectively) and are therefore excluded from the target set.

Second, we required that candidate UPR targets exhibit inductions that differ between wild-type and UPR-deficient mutant samples at a level of significance (3.6 standard deviations) corresponding to a difference that would occur by chance less than one time in 6400, i.e., less than one gene in the *S. cerevisiae* genome. Finally, in order to eliminate ORFs that passed the criteria established above due solely to decreases in expression in the UPR-deficient mutants, we required that UPR targets show a mean change in the wild-type of greater than 1.5-fold. The set of genes satisfying these criteria defines the *HAC1*- and *IRE1*-dependent response to ER protein misfolding.

Two genes that are known targets of the UPR (*KAR2* and *INO1*) did not pass the strict statistical criterion (2.75 and 3.0 standard deviations, respectively) due to significant residual upregulation in the mutant strains, as previously observed (Cox et al., 1993). Thus, the high stringency of the criteria employed results in an underestimation of the full scope of the UPR. Despite this stringent selection, we identified a large set comprised of 381 ORFs that are induced by both DTT and tunicamycin in an *IRE1*- and *HAC1*-dependent manner. A database containing the complete data set can be found at http://www.cell.com/cgi/content/full/101/3/249/DC1. We have also included transcriptional data from a strain deleted for *OPI1*, a negative regulator of inositol and membrane biosynthesis that is inhibited upon activation of *HAC1* (Cox et al., 1997). These data reveal that loss of *OPI1* leads to induction of only a small subset of UPR target genes. We conclude that the vast majority of UPR target genes defined here are not upregulated as a secondary consequence of membrane proliferation.

For every ORF, we then determined the UPR-dependent induction due to a particular unfolding treatment (DTT or tunicamycin) by dividing the average fold change resulting from that treatment in wild-type cells by the average fold change in the UPR-deficient mutants. A scatter plot of DTT induction versus the tunicamycin induction (Figure 1C) reveals that, as with known UPR targets, the newly identified targets of the UPR (red points) are induced to similar levels by DTT and tunicamycin. Because the two unfolding agents have similar effects on gene expression, we projected this scatter plot onto the diagonal (equal induction by DTT and tunicamycin) and took the distance along this line as a measure of combined DTT and tunicamycin induction. This analysis provides a single metric of UPR-dependent induction by the two unfolding agents. A histogram of this

Table 1. Secretory Pathway Genes Upregulated by the UPR

TRANSLOCATION	
Translocon	*SEC61, SBH1, SLS1*
Posttranslational translocation	*SEC62, SEC71, SEC72*
Signal peptidase	*SPC2*
GLYCOSYLATION/MODIFICATION	
Core oligosaccharide synthesis	*DPM1, PMI40, RHK1, SEC59*
Oligosaccharyltransferase	*OST2, OST3, SWP1, WBP1*
Glycoprotein processing	*ALG6, ALG7, MNS1, RAM2, STE24*
GPI anchoring	*GAA1, GPI12, LAS21, MCD4*
Golgi/O-linked glycosylation	*KTR1, MNN11, PMT1, PMT2, PMT3, PMT5*
PROTEIN FOLDING	
Chaperones	*FKB2, JEM1, LHS1, SCJ1, YFR041C*[a]
Disulfide bond formation	*ERO1, EUG1, MPD1, MPD2, PDI1*
PROTEIN DEGRADATION	
ER-associated degradation (ERAD)	*DER1, HRD1/DER3, HRD3, UBC7*
Ubiquitin/proteasome	*DOA4, PEX4*
VESICLE TRAFFICKING/TRANSPORT	
Budding (ER-Golgi)	*ERV25, SEC12, SEC13, SEC16, SEC24, SED4, SFB2, SFB3, YMR040W*[b]
Fusion (ER-Golgi)	*BOS1, TRS120*
Retrieval (Golgi-ER)	*ERD2, RER2, RET2, SEC26, SEC27*
Distal secretion	*APL3, ARL3, BFR1, MYO5, SEC6, TUS1, YPT10*
LIPID/INOSITOL METABOLISM	
Fatty acid metabolism	*ACB1, HAP1, MGA2, YJR107W*[c]
Heme biosynthesis	*DFR1, HEM12, HEM13, HEM15, RIB1*
Phospholipid biosynthesis	*EPT1, INP51, LPP1, OP13, SCS3, SLC1*
Sphingolipid biosynthesis	*LCB1*
Sterol metabolism	*ARE1, HMG2, YHR073W*[d]
VACUOLAR PROTEIN SORTING	*LUV1, STP22, VPS17, VPS35*
CELL WALL BIOGENESIS	*CHS7, CSR1, ECM3, ECM8, ECM31, EXG2, GAS5, PKC1, SPF1, YKR027W*[e], *YOR239W*[f]

Bold headings correspond to functional categories illustrated in Figure 2. Genes are assigned to subcategories according to summaries of published data listed in the *Saccharomyces* Genome Database (SGD) and Yeast Protein Database (YPD).
[a] DnaJ homolog with predicted signal sequence. [b] Homolog of BAP-29 and BAP-31, sorting proteins that control anterograde transport of certain membrane proteins from the ER to the Golgi complex (Ng et al., 1997). [c] Homolog of acylglycerol lipase. [d] Homolog of human oxysterol-binding protein (OSBP). [e] Homolog of Chs6p, involved in localization of Chs3p. [f] Homolog of Chs5p, required for protease activation of Chs3p.

metric for all ORFs (Figure 1D) displays a significant degree of asymmetry, with the newly identified UPR targets (red bars) corresponding to the excess ORFs on the right side of the distribution. The fact that there is not a corresponding set of ORFs on the left side of the histogram indicates that the UPR is largely an inductive transcriptional response, with little specific repression.

Many Aspects of Secretory Function Are Regulated by the UPR

Our analysis reveals that the scope of the UPR is far broader than anticipated by the functions of previously reported target genes. The 381 ORFs that passed our criteria include 208 genes for which some functional information is available (named genes or their homologs) and 173 genes for which no information is presently available. Of the functionally characterized genes, 103 are known or predicted by sequence homology to play roles in secretion or the biogenesis of secretory organelles. As expected, we observe induction of ER-resident chaperones and genes involved in phospholipid metabolism. However, these represent only a fraction of this set of target genes, which also includes several categories of genes with functions throughout the secretory pathway (Figure 2). These functional categories (detailed in Table 1) include translocation, protein glycosylation, vesicular transport, cell wall biosynthesis, vacuolar protein targeting, and ER-associated degradation.

The UPR Controls the Rate of ERAD

The induction of ERAD components was particularly intriguing, as it suggested coordination between the UPR and another pathway related to protein misfolding in the ER. We confirmed the genomic array measurements of ERAD gene expression levels by Northern blot analysis and found that the results were in good agreement. *DER1* and *HRD3*, nonessential genes required for ERAD, are strongly induced upon tunicamycin treatment of wild-type cells but not Δ*ire1* mutant cells (Figure 3). *SEC61*, an essential component of the translocon also required for ERAD (Pilon et al., 1997; Plemper et al., 1997; Zhou and Schekman, 1999), is similarly induced in an *IRE1*-dependent manner. In contrast, transcription of *SRP54*, which is also important for protein translocation but not known to influence the rate of ERAD, is unresponsive to tunicamycin treatment.

Since several genes important for ERAD are induced by the UPR, we examined candidate genes to identify novel ERAD components. One of these candidates, *YOL031c*, was chosen on the basis of its homology to a *Yarrowia lipolytica* gene (*SLS1*) that encodes a nonessential ER-lumenal protein that is physically associated with the translocon (Boisramé et al., 1999). Hereafter, we refer to this gene as *PER100* (*p*rotein *p*rocessing in the *ER*; Ng et al., submitted).

We measured ERAD rates using strains expressing CPY* (*prc1-1*), a constitutively misfolded soluble secretory protein and a well-characterized substrate for ERAD

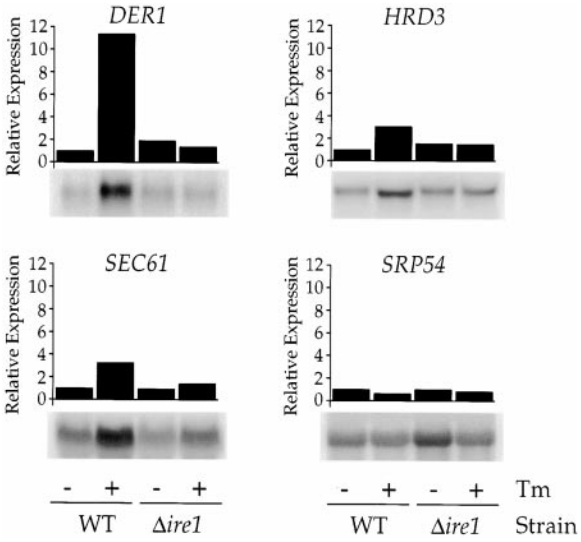

Figure 3. Northern Blot Analysis Confirms UPR-Dependent Induction of Genes Involved in ERAD

Northern blot analysis was performed on the same RNA samples that were used to collect the microarray data for cells treated with tunicamycin (Tm) for 60 min. Shown are data for *DER1* and *HRD3*, encoding dedicated ERAD components; *SEC61*, encoding a protein shared with the general translocation machinery; and *SRP54*, which is involved in translocation but not ERAD. All expression levels were normalized against the *ACT1* message levels and then against the expression level for the untreated wild-type sample. For comparison, the microarray data for wild-type cells treated with tunicamycin (Tm) found 3.9-, 3.4-, 2-, and 0.66-fold changes compared to untreated cells for *DER1*, *HRD3*, *SEC61*, and *SRP54*, respectively.

(Knop et al., 1996). To facilitate immunoprecipitation of CPY*, the *prc1-1* gene, which was driven by its native (*PRC1*) promoter, was modified by addition of sequences encoding a C-terminal HA tag (Ng et al., submitted). In each of the experiments described below, we pulse-labeled cells with ^{35}S-methionine/cysteine, chased over a 45 min time course, immunoprecipitated with antibodies against the HA epitope, and subjected samples to SDS-PAGE and autoradiography. The rate of disappearance of CPY* represents the rate of ERAD.

We compared the rate of degradation of CPY* in a Δ*per100* mutant to the rate in wild-type cells and in the Δ*der1* mutant, in which ERAD is completely blocked (Knop et al., 1996). In wild-type cells, CPY* was degraded with a half-life of 15 ± 1 min (Figure 4A, squares), a value in agreement with published observations. As anticipated, a Δ*der1* mutant failed to measurably degrade CPY* over the time course (Figure 4A, diamonds). The Δ*per100* mutant displayed an intermediate phenotype, with a CPY* half-life of 24 ± 2 min (Figure 4A, triangles). This stabilization is roughly comparable to that reported for strains containing ERAD-deficient alleles of *KAR2* (Plemper et al., 1997) and deletion of the *PMR1* ion transporter, also required for wild-type levels of ERAD (Dürr et al., 1998). Thus, the *PER100* gene product plays a role in maintaining efficient ERAD, perhaps through an activity at the translocon.

Because several UPR target genes are required for ERAD, we asked whether mutant strains unable to induce the UPR are also deficient in ERAD. Indeed, the Δ*ire1* mutant degraded CPY* at a reduced rate (half-life of 25 ± 1 min, as compared to 15 ± 1 min in wild-type cells; Figure 4B, circles). Given that an intact UPR is necessary for efficient ERAD, we asked whether activation of the UPR is sufficient to increase the rate of degradation. We constructed strains bearing a plasmid system in which the spliced form of the *HAC1* gene is driven by a glucocorticoid-responsive element (GRE)-containing promoter; the GRE-*HAC1* gene and the glucocorticoid receptor, a ligand-regulated transcriptional activator, are expressed in *trans* on separate high copy (2μ) plasmids. This system allowed us to induce the UPR by expressing Hac1p upon addition of the glucocorticoid receptor ligand deoxycorticosterone (DOC). After 90 min of exposure to DOC, steady-state levels of Hac1p reached a plateau, resulting in significant induction of several UPR target genes tested by Northern blot (data not shown). The rate of CPY* degradation was dramatically increased in cells bearing GRE-*HAC1* and treated with DOC (half-life of 6 ± 1 min; Figure 4C, diamonds) compared to DOC-treated cells bearing the GRE vector alone (half-life of 30 ± 2 min; Figure 4C, squares). Cells bearing the GRE vector alone degrade CPY* more slowly than do the wild-type cells used in Figures 4A and 4B; this difference may be explained by the diminished growth rate we observe for these strains, which bear multiple 2μ plasmids. In any event, degradation of CPY* is accelerated in the DOC-induced samples expressing *HAC1* even when compared to the wild-type samples displayed in Figure 4A and 4B.

In the GRE-inducible system, *HAC1*-expressing cells induce UPR target genes in the absence of high levels of unfolded protein. We also measured ERAD after activating the UPR in wild-type cells with chemical agents that interfere with protein folding. In marked contrast to the above experiments, in cells treated with tunicamycin (Figure 4D, circles) or DTT (Figure 4D, diamonds) for 1 hr prior to pulse labeling, ERAD was completely blocked. These treatments generate pathologically high levels of misfolded protein; the blockage of ERAD may therefore result from saturation of the capacity of the ERAD system despite activation of the UPR and transcriptional upregulation of several ERAD components under these conditions (see the Discussion). Consistent with this, expression of high levels of a single misfolded protein results in slower ERAD: cells expressing CPY* from the strong promoter *TDH3* grow at a normal rate but degrade CPY* with significantly slower kinetics than when the protein is expressed under control of the native (*PRC1*) promoter (half-life of 30±1 min; Figure 4D, triangles).

Mutations in ERAD Components Result in Constitutive Activation of the UPR

Previous work has indicated that mutations in genes required for ERAD do not cause a detectable growth phenotype under normal growth conditions (Knop et al., 1996). While it is possible that this is the case because degradation of misfolded proteins is required for life only under conditions of extreme folding stress, an alternative explanation is that the UPR can compensate for a defect in ERAD, eliminating misfolded proteins by other means. In the latter case, a loss of ERAD function would result in an accumulation of unfolded proteins in the ER and chronic activation of the UPR.

We tested for constitutive activation of the UPR in

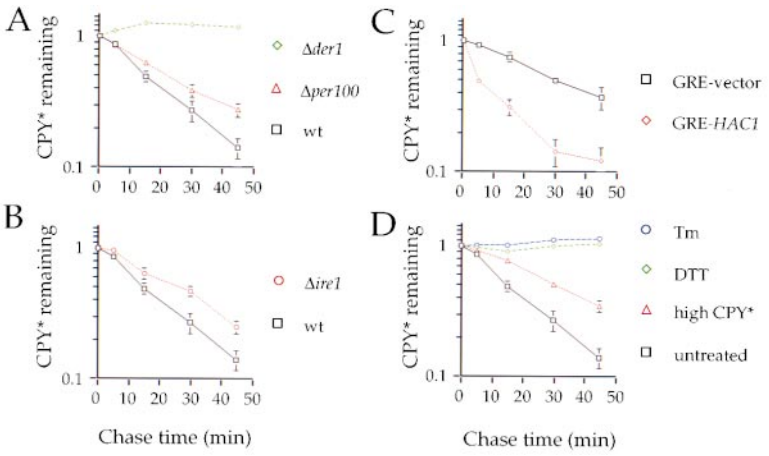

Figure 4. The Rate of Degradation of CPY* Is Controlled by the UPR

Cells expressing an HA-tagged copy of CPY* were ^{35}S-radiolabeled and then chased for the indicated time. The rate of degradation of CPY* was analyzed by immunoprecipitation followed by SDS-PAGE and autoradiography. Quantitation of CPY*, normalized against intensity in the time = 0 sample, was plotted against chase time, and a half-life (see text) computed by fitting a single exponential curve to each graph. Error bars indicate standard deviation from the average of four (A, B, and D) or three (C) independent experiments. Shown is the comparison of the rate of CPY* degradation in:

(A) Cells deleted for the known ERAD component *DER1* (Δ*der1*) or *PER100* (Δ*per100*) versus wild-type cells (WT).

(B) Cells deleted for *IRE1* (Δ*ire1*) versus wild-type cells (WT).

(C) Cells expressing Hac1p under control of the glucocorticoid-responsive promoter (GRE-*HAC1*) versus cells not expressing Hac1p (GRE-vector). Both samples were treated with DOC for 90 min prior to pulse labeling.

(D) Cells treated with DTT or tunicamycin (Tm) or expressing CPY* under control of the strong promoter *TDH3* (high CPY*) versus a control (untreated).

cells lacking *DER1*, *HRD1*, *HRD3*, or the newly identified ERAD gene *PER100* using a sensitive reporter of UPR activation. The reporter construct consists of the gene encoding green fluorescent protein (GFP) driven by four repeats of the unfolded protein response element from the *KAR2* promoter (UPRE; Cox and Walter, 1996; Mori et al., 1996). Comparison of steady-state levels of GFP fluorescence in Δ*der1*, Δ*hrd1*, Δ*hrd3*, and Δ*per100* strains to those of wild-type cells (Figure 5A, left panel) reveals a ~2-fold induction of the UPR under normal growth conditions in these mutants. Both wild-type and ERAD-deficient cells showed similar levels of maximal GFP expression under DTT treatment (Figure 5A, right panel), indicating that the observed induction of the UPR is not the result of a nonspecific increase in GFP levels in the mutant cells.

Mutations in the UPR and ERAD Are Synthetically Lethal

We have thus far demonstrated that the rate of ERAD is modestly decreased in the absence of a functional UPR (Figure 4B). In addition, ERAD-deficient cells show a constitutive, partial activation of the UPR. Together, these data suggest that the UPR and ERAD cooperate to eliminate misfolded proteins under normal growth conditions, predicting that simultaneous loss of both pathways should be more detrimental to the cell than the loss of either one alone.

To test for such synthetic effects, we constructed diploid strains containing heterozygous deletions in *IRE1* as well as one of the previously identified genes required for ERAD (*DER1*, *HRD1*, or *HRD3*) or the newly identified ERAD gene *PER100*. Following meiosis, spores bearing both Δ*ire1* and Δ*der1* mutations germinated normally but failed to grow at 37°C (Figure 5B). By contrast, the single mutants showed no growth defect under either condition. Consistent with the fact that there is a broader spectrum of substrates that are dependent on Hrd1p and Hrd3p for their ERAD-mediated degradation (Hampton et al., 1996; Knop et al., 1996), spores bearing both Δ*ire1* and either Δ*hrd1* or Δ*hrd3* mutations displayed a stronger phenotype than the Δ*ire* Δ*der1* spores. These strains showed poor viability following meiosis, grew irregularly at room temperature, and entirely failed to grow at 37°C (Figure 5B). Similarly, strains containing deletions in both the *IRE1* and *PER100* genes failed to grow beyond the few cell stage despite the fact that loss of *PER100* alone caused little or no growth defect (data not shown).

Discussion

Using high-density oligonucleotide arrays in conjunction with strains bearing specific defects in the UPR, we have defined the transcriptional scope of the UPR. Remarkably, the UPR affects virtually every stage of the secretory pathway. From entry into the ER (translocation), through processing (folding, covalent modification, and sorting), until exit from the pathway (arrival at a target organelle, secretion from the cell, or degradation), a secretory protein's progress is influenced by the transcriptional targets of the UPR. The breadth of this response suggests that genes involved in many secretory functions, including but not limited to ER-resident chaperones, are required for maintenance of the specialized protein folding environment.

The scope of the UPR is focused in large part on the secretory pathway, with approximately half of the 208 UPR target genes for which functional data are available playing roles in secretion. The 173 transcriptional targets of the UPR with no known function are therefore excellent candidates for genes with important secretory functions. Indeed, our expression data and functional studies allowed us to identify the previously uncharacterized *S. cerevisiae* homolog of the *Y. lipolytica* gene *SLS1*, referred to above as *PER100*, as a novel component required for efficient ERAD.

Despite its breadth, the UPR results in a specific remodeling of the secretory pathway rather than the indiscriminate upregulation of all ER or secretory pathway

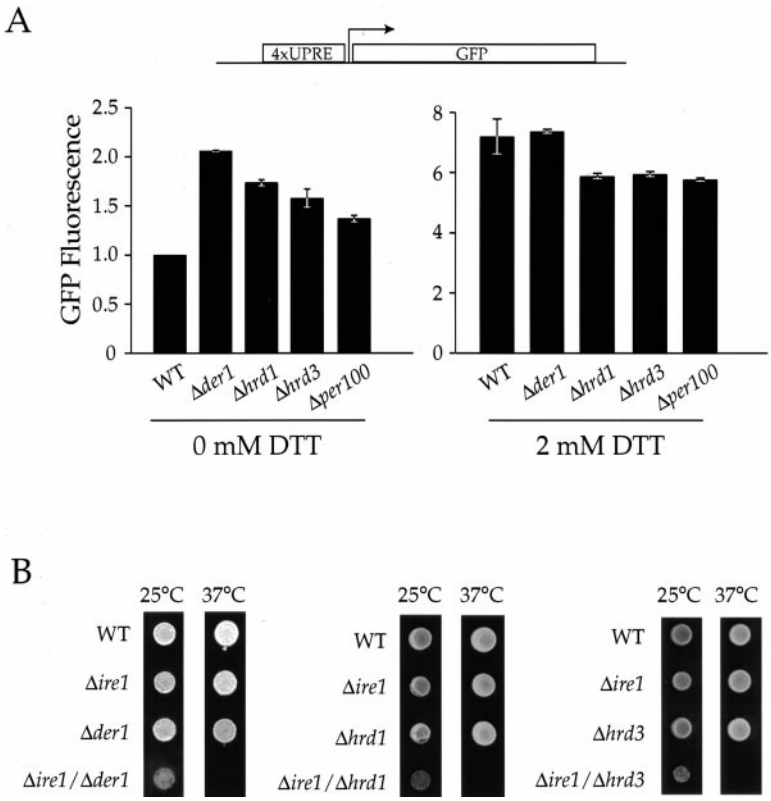

Figure 5. Genetic Interaction between Mutations in UPR and ERAD Genes

(A) Deletion of genes involved in ERAD potentiates the UPR. Cells contained an integrated reporter gene in which GFP was driven by four copies of the unfolded protein response element (UPRE). Wild-type cells (WT), cells deleted for one of the known ERAD components *DER1* (Δ*der1*), *HRD1* (Δ*hrd1*), or *HRD3* (Δ*hrd3*), as well as cells deleted for *PER100* (Δ*per100*) were grown to mid-log phase and analyzed for GFP expression by FACS. Shown on the left is the mean GFP fluorescence for each strain. Strains were analyzed for constitutive expression of GFP ("0 mM DTT") or UPR-induced expression after exposure to 2 mM DTT for 90 min ("2 mM DTT").

(B) Deletion of genes involved in ERAD is synthetically lethal with absence of the UPR. The indicated yeast strains bearing either a single deletion in one of three well-characterized ERAD genes (*DER1*, *HRD1*, or *HRD3*) or this deletion combined with a deletion of *IRE1* were plated at 25°C and 37°C. For comparison, a strain bearing a deletion of *IRE1* and an isogenic parent (WT) are shown. In all cases, roughly equal numbers of cells were spotted.

components. For example, many components of the COP-II vesicle coat involved in ER-Golgi trafficking are targets, including two strongly induced homologs of *SEC24* that have been suggested to play a role in export of specific cargo proteins (Roberg et al., 1999). In contrast, components of the COP-I/"coatomer" involved in retrograde transport are less well represented, and those that are regulated by the UPR typically show only modest induction. Similarly, of the ER-resident chaperones involved in folding or secretion of specific substrates (Ellgaard et al., 1999), only *CHS7*, required for maturation of chitin synthase III (Trilla et al., 1999), is upregulated. This specificity suggests that rather than merely increasing the capacity of the secretory pathway, the UPR results in selective induction of those activities that are essential under folding stress, e.g., in the cases mentioned above, enhanced anterograde transport of a particular subset of secretory proteins, or folding of proteins involved in maintaining cell wall integrity. The set of UPR target genes may therefore specify those activities required to optimize protein folding in the ER.

How might the set of UPR target genes act in a concerted manner to promote efficient folding? An attractive hypothesis is that a critical function of the UPR is to reduce the lumenal concentration of misfolded protein, by either directly refolding proteins or removing them from the ER (Figure 6). In this model, abundant chaperones would bind to misfolded species, prevent aggregation, and promote folding. Similarly, glycosylation enzymes would assist in the folding of proteins that require carbohydrate modification to attain their proper conformation. Consistent with this suggestion, we found in an independent study that mutations that compromise either addition of GPI anchors or protein glycosylation are lethal in the absence of UPR function (Ng et al., submitted). Moreover, UPR induction in mammalian cells was recently shown to accelerate synthesis of the dolichol-oligosaccharides employed in N-linked glycosylation (Doerrler and Lehrman, 1999). In the event that direct attempts to increase the efficiency of folding fail, induction of specific COP-II components might enable efficient packaging of cargo proteins (possibly including unfolded proteins) into anterograde vesicles or simply increase the overall capacity of anterograde transport. Such an increase in secretory capacity might facilitate targeting of misfolded species to the vacuole for degradation (Hong et al., 1996), consistent with our observation that several genes involved in vacuolar targeting are also UPR targets. Similarly, induction of phospholipid biosynthetic enzymes would generate new membranes, thereby increasing the volume of the ER, simultaneously diluting unfolded proteins and preparing the compartment to receive an influx of newly synthesized folding factors. Finally, induction of ERAD components directly enhances the clearance of misfolded proteins from the ER to the cytosol.

Our functional studies demonstrate that the capacity of the ERAD system is readily saturated under conditions of ER stress and that the UPR plays a direct role in counteracting this saturation. We find that the UPR is necessary for efficient ERAD function, as UPR-deficient cells degrade CPY* at a reduced rate; these results are in qualitative agreement with recent reports that both full-length CPY* (Ng et al., submitted) and a truncated allele of CPY* (Casagrande et al., 2000 [April issue of *Molecular Cell*]) are stabilized in the Δ*ire1* mutant. This

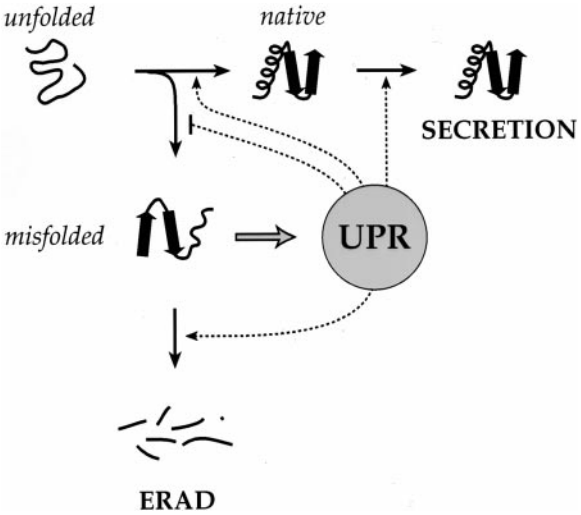

Figure 6. Schematic Model Illustrating the Coordinated Action of the UPR and ERAD

Proteins enter the ER in an unfolded form, whereupon they either fold, oligomerize, and pass on to the later secretory pathway or become irreversibly misfolded and are eliminated by the ERAD machinery. Either cellular stress or loss of ERAD results in accumulation of misfolded proteins and thereby activation of the UPR (filled-in arrow). The UPR acts to reduce levels of misfolded proteins by enhancing folding to the native state, promoting transit to the distal secretory pathway, and enhancing the rate of ERAD, while simultaneously reducing the formation of misfolded species.

decrease in ERAD rate is likely to result from chronic misfolding in Δ*ire1* strains rather than from direct loss of the ERAD machinery, as Δ*ire1* cells do not show decreased basal transcription of ERAD genes (Figure 3). The notion that ERAD capacity can be readily saturated is further supported by the observation that treatment with DTT or tunicamycin, both of which generate high levels of unfolded ER proteins, dramatically decreases the rate of CPY* degradation. High levels of even a single misfolded protein can substantially decrease the rate of degradation: expression of CPY* from a strong promoter resulted in accumulation of the protein and a doubling of its half-life, consistent with the idea that ERAD capacity can be saturated by high concentrations of substrate. In striking contrast to the DTT and tunicamycin treatments, we find that when the UPR is induced by expression of Hac1p, which does not cause accumulation of unfolded proteins, the rate of ERAD is significantly increased, thus demonstrating that the UPR plays a direct role in enhancing ERAD. It has recently been postulated that the rate-limiting step in the degradation of a protein through ERAD is the conversion of N-linked oligosaccharide from the Man9 to the Man8 form (Jakob et al., 1998), a reaction catalyzed by the glycosylase Mns1p. We found that UPR activation results in the upregulation of *MNS1*, raising the intriguing possibility that the UPR accelerates ERAD in part via increased expression of an enzyme that catalyzes the rate-limiting step; in this scenario, during times of folding stress, activation of the UPR would reduce the time available for a protein to fold before being targeted for degradation.

Although the UPR enhances ER degradation capacity under acute folding stress, the ERAD pathway also plays a critical and previously undescribed role in the disposal of misfolded proteins even under normal growth conditions. Loss of ERAD function in Δ*der1*, Δ*hrd1*, Δ*hrd3*, and Δ*per100* strains leads to chronic accumulation of unfolded proteins in the ER, as evidenced by constitutive activation of the UPR. Recently, Zhou and Schekman (1999) reported that *SEC61* alleles with specific defects in ERAD, as well as deletion of several other ERAD components, also cause constitutive UPR induction. Thus, the chronic accumulation of misfolded proteins in the ER appears to be a general consequence of loss of ERAD. Earlier studies suggested that even if it were constitutively active, ERAD has little physiological importance in the absence of an acute stress, as loss of ERAD function does not lead to a detectable growth phenotype (Knop et al., 1996; Zhou and Schekman, 1999). Here, we show that this lack of phenotype results from a compensatory effect of UPR induction: deletion of any of three well-characterized ER-resident ERAD components (*DER1*, *HRD1*, *HRD3*) or the newly identified ERAD component *PER100* results in dramatic loss of viability in a Δ*ire1* strain. In a parallel study, we found that deletion of either of two genes encoding cytosolic ERAD components, the membrane-bound ubiquitin-conjugating enzyme Ubc7p and the proteasome regulator Son1p/Rpn4p, also shows a synthetic lethal phenotype when combined with loss of *IRE1* (Ng et al., submitted). Hence, loss of ERAD function at any location (ER lumen, ER membrane, or proteasome) results in a requirement for UPR-mediated clearance of misfolded proteins.

Taken together, our observations argue that a fraction of the proteins passing through the ER will inevitably misfold and that removal of these misfolded polypeptides is an essential process under all growth conditions. The chronic misfolding of proteins in the ER is likely to reflect the inherent difficulty of folding secretory and membrane proteins, which unlike cytosolic proteins often require covalent modifications, such as disulfide bonds and glycosylation, as well as the precise ordering of transmembrane domains across and within the lipid bilayer. In the absence of a functional UPR, the ERAD capacity is sufficient to dispose of this flux provided the cell does not face an unusual stress. Conversely, when the UPR is available in a cell with diminished ERAD capacity, misfolded proteins can still be handled by multiple mechanisms, including refolding by chaperones, clearance from the ER by anterograde vesicular transport, or an alternate means of degradation, e.g., in the vacuole or by the action of other UPR-induced ERAD genes. Thus, the UPR and ERAD represent partially overlapping or compensatory means to the same essential end: elimination of misfolded secretory proteins, which are inevitably generated during the course of normal growth.

Experimental Procedures

General Procedures

Yeast manipulations were performed using standard methods (Sherman, 1991), except that the pH of YPD was lowered to that of synthetic defined media (pH = 5.4) to inhibit oxidation of DTT. All incubations were at 30°C, unless otherwise indicated.

Plasmid Construction

Plasmid pRS425-GRE, which contains the glucocorticoid responsive element upstream of a multiple cloning site, was generated by subcloning the XhoI-SacI fragment of p2UG (Schena et al., 1991) into the corresponding sites of pRS425 (Sikorski and Hieter, 1991). Plasmid pCP274, which contains the spliced form of the *HAC1* gene downstream of the GRE promoter, was generated by cloning the DraI/SmaI fragment of pRC43 (Cox et al., 1997) into the SmaI cloning site of pRS425-GRE. Plasmid pKT058, which encodes a GFP reporter gene driven by four repeats of the *KAR2* UPRE, was generated by subcloning the UPRE- and GFP-containing ClaI-SacI fragment of pKT007 (Pollard et al., 1998) into pRS304 (Sikorski and Hieter, 1991). Plasmid pCP280, which contains the *prc1-1* gene encoding CPY* under control of the *TDH3* promoter, was constructed by ligating a blunted AccI fragment of pDN431 (Ng et al., submitted) into blunted, BamHI-linearized pG-1 (2μ TRP1; Schena et al., 1991).

Yeast Strains

The wild-type strains W303-1B and JC103 (which was derived from W303-1B by integration of a β-gal UPR reporter into the *HIS3* and *LEU2* loci), the Δ*ire1* strain CS165, and the Δ*hac1* strain JC408 are as described (Cox et al., 1993; Cox and Walter, 1996). The *PER100*, *HRD1*, and *HRD3* deletion strains were derived from a W303-1B parent by replacing the entire open reading frame of each gene with an auxotrophic marker (*LEU2* for *PER100* or *HIS3* for *HRD1* and *HRD3*) using the method of Pringle and coworkers (Longtine et al., 1998). Strains used in the experiments described in Figure 4D were W303-1B transformed with pT2.GN795 (Schena et al., 1991), which contains the glucocorticoid receptor under control of the GPD promoter and either pRS425-GRE ("GRE-vector") or pCP274 ("GRE-*HAC1*").

Genomic Arrays: Sample Preparation and Hybridization

Biotinylated cRNA samples were prepared and processed largely as described previously (Wodicka et al., 1997). In brief, cultures of wild-type (JC103), CS165, or JC408 strains were grown to mid-log phase in rich medium and treated with either 1 μg/ml tunicamycin (Tm) or 2 mM DTT. At the indicated times, cells were treated with 20 mM azide, recovered from 250 ml aliquots by centrifugation, and frozen in liquid nitrogen. Total RNAs were prepared by freeze/thaw/hot phenol extraction (Schmitt et al., 1990), and mRNA was purified using the PolyATtract system (Promega) according to the manufacturer's instructions. First-strand cDNA synthesis was performed using AMV (Promega) according to the manufacturer's instructions. Second-strand syntheses, cRNA amplifications, fragmentations, and hybridizations were conducted as described previously (Wodicka et al., 1997).

Data Analysis and Categorization

For each treatment condition, fold changes in mRNA levels relative to untreated cultures were determined using the GeneChip software package (Wodicka et al., 1997). For all subsequent analyses, the base 2 logarithm ($\log_2$) of the fold changes was utilized. For each ORF, the expression pattern was represented by a nine component vector composed of the following elements: <WT.D.15, WT.D.30, WT.D.60, WT.D.120, WT.T.60, Δ*ire1*.D.60, Δ*ire1*.T.60, Δ*hac1*.D.60, and Δ*hac1*.T.60>. The first segment of each element indicates the strain, the second the treatment condition (DTT [D] or Tm [T]), and the third the treatment time (i.e., Δ*ire1*.D.60 is the $\log_2$ of the fold change in a Δ*ire1* strain treated with DTT for 60 min compared to the untreated Δ*ire1* strain). An expression vector representing the canonical response profile was generated by averaging the vectors from seven known UPR targets: *KAR2*, *EUG1*, *PDI1*, *LHS1*, *FKB2*, *ERO1*, and *INO1*. Pearson correlations between a given ORF's vector and the canonical profile were calculated (Eisen et al., 1998). ORFs with a Pearson correlation coefficient at least as great as that of *KAR2* (P = 0.81) were subjected to a Z test with a null hypothesis of no difference between the five treatments of the wild-type strain and four treatments for the UPR-deficient strains. ORFs with a Z score of greater than 3.6, corresponding to a chance occurrence of approximately 1 in 6400, were called as UPR targets provided that the average induction of the wild-type strain was greater than 1.5. Assignment of known/named ORFs to functional categories followed curated data available online at SGD (http://genome-www.stanford.edu/Saccharomyces).

The calculation of UPR-dependent DTT induction used in Figure 1C is:

$$\frac{1}{4}\left((\text{WT.D.15}) + (\text{WT.D.30}) + (\text{WT.D.60}) + (\text{WT.D.120})\right) - \frac{1}{2}\left((\Delta ire1\text{.D.60}) + (\Delta hac1\text{.D.60})\right)$$

The calculation of UPR-dependent tunicamycin induction used in Figure 1C is:

$$(\text{WT.T.60}) - \frac{1}{2}\left((\Delta ire1\text{.T.60}) + (\Delta hac1\text{.T.60})\right)$$

CPY* Degradation Assay

Strains bearing a low copy CPY*-HA expression plasmid (Ng et al., submitted) were grown to OD_{600} = 1.0. Cell pellets were washed twice, resuspended at 3 OD/ml in medium lacking methionine, and incubated for 1 hr at 30°C with 1 μg/ml tunicamycin, 2 mM DTT, or 100 μM DOC as indicated. Newly synthesized polypeptides were pulse labeled by addition of 20 μCi/OD ProMix (Amersham) for 20 min and chased by addition of 2 mM each cold methionine and cysteine. Time points were taken by transferring 1 ml aliquots into chilled tubes containing 100 ml 100% TCA and 3 μl 3M sodium azide and freezing immediately in liquid nitrogen. Immunoprecipitations were performed by the method of Gaynor et al. (1994) except that after preclearing, supernatants were incubated for 4 hr at 4°C with 7 μl of 16B11 anti-HA antibody (BAbCo) and immunoprecipitated by addition of 1 μl rabbit anti-mouse antibody (Jackson) and 25 μl protein A-Sepharose slurry and incubation for 30 min.

FACS Analysis

Strains containing an integrated UPRE-GFP reporter were constructed by transforming W303-1B (wild-type), Δ*der1*, Δ*hrd1*, and Δ*hrd3* with EcoRV-linearized pKT007 or by transforming Δ*per100* with EcoRV-linearized pKT058. Integrations were confirmed by genomic PCR analysis. All strains were grown to mid-log phase (OD_{600} = 0.5) and then cultures were grown in the presence or absence of 2 mM DTT for 1.5 hr to induce the UPR. GFP fluorescence was measured by FACS analysis on a FACScan instrument (Becton-Dickinson).

Acknowledgments

The authors wish to thank Bruce Conklin and Chandi Griffin of the San Francisco General Hospital Genomics Center for invaluable assistance with the genomic array data collection, and Davis Ng and Vladimir Denic for valuable discussions. C. P. is supported by a Howard Hughes Predoctoral fellowship. This work was supported by grants from the National Institutes of Health (P. W. and J. S. W.), Searle Scholar Program (J. S. W.), and the David and Lucille Packard Foundation (J. S. W.). P. W. is an investigator of the Howard Hughes Medical Institute.

Received January 13, 2000; revised March 30, 2000.

References

Biederer, T., Volkwein, C., and Sommer, T. (1997). Role of Cue1p in ubiquitination and degradation at the ER surface. Science *278*, 1806–1809.

Boisramé, A., Beckerich, J.M., and Gaillardin, C. (1999). A mutation in the secretion pathway of the yeast Yarrowia lipolytica that displays synthetic lethality in combination with a mutation affecting the signal recognition particle. Mol. Gen. Genet. *261*, 601–609.

Bonifacino, J.S., and Weissman, A.M. (1998). Ubiquitin and the control of protein fate in the secretory and endocytic pathways. Annu. Rev. Cell. Dev. Biol. *14*, 19–57.

Bordallo, J., Plemper, R.K., Finger, A., and Wolf, D.H. (1998). Der3p/

Hrd1p is required for endoplasmic reticulum-associated degradation of misfolded lumenal and integral membrane proteins. Mol. Biol. Cell. *9*, 209–222.

Casagrande, R., Stern, P., Diehn, M., Shamu, C., Osario, M., Zuñiga, M., Brown, P.O., and Ploegh, H. (2000). Degradation of proteins from the ER of *S. cerevisiae* requires an intact unfolded protein response pathway. Molecular Cell *5*, 729–735.

Chapman, R., Sidrauski, C., and Walter, P. (1998). Intracellular signaling from the endoplasmic reticulum to the nucleus. Annu. Rev. Cell. Dev. Biol. *14*, 459–485.

Cox, J.S., and Walter, P. (1996). A novel mechanism for regulating activity of a transcription factor that controls the unfolded protein response. Cell *87*, 391–404.

Cox, J.S., Shamu, C.E., and Walter, P. (1993). Transcriptional induction of genes encoding endoplasmic reticulum resident proteins requires a transmembrane protein kinase. Cell *73*, 1197–1206.

Cox, J.S., Chapman, R.E., and Walter, P. (1997). The unfolded protein response coordinates the production of endoplasmic reticulum protein and endoplasmic reticulum membrane. Mol. Biol. Cell. *8*, 1805–1814.

Doerrler, W.T., and Lehrman, M.A. (1999). Regulation of the dolichol pathway in human fibroblasts by the endoplasmic reticulum unfolded protein response. Proc. Natl. Acad. Sci. USA *96*, 13050–13055.

Dürr, G., Strayle, J., Plemper, R., Elbs, S., Klee, S.K., Catty, P., Wolf, D.H., and Rudolph, H.K. (1998). The medial-Golgi ion pump Pmr1 supplies the yeast secretory pathway with Ca2+ and Mn2+ required for glycosylation, sorting, and endoplasmic reticulum-associated protein degradation. Mol. Biol. Cell. *9*, 1149–1162.

Eisen, M.B., Spellman, P.T., Brown, P.O., and Botstein, D. (1998). Cluster analysis and display of genome-wide expression patterns. Proc. Natl. Acad. Sci. USA *95*, 14863–14868.

Ellgaard, L., Molinari, M., and Helenius, A. (1999). Setting the standards: quality control in the secretory pathway. Science *286*, 1882–1888.

Gaynor, E.C., te Heesen, S., Graham, T.R., Aebi, M., and Emr, S.D. (1994). Signal-mediated retrieval of a membrane protein from the Golgi to the ER in yeast. J. Cell Biol. *127*, 653–665.

Hampton, R.Y., Gardner, R.G., and Rine, J. (1996). Role of 26S proteasome and HRD genes in the degradation of 3-hydroxy-3-methylglutaryl-CoA reductase, an integral endoplasmic reticulum membrane protein. Mol. Biol. Cell *7*, 2029–2044.

Hiller, M., Finger, A., Schweiger, M., and Wolf, D. (1996). ER degradation of a misfolded luminal protein by the cytosolic ubiquitin-proteasome pathway. Science *273*, 1725–1728.

Hong, E., Davidson, A.R., and Kaiser, C.A. (1996). A pathway for targeting soluble misfolded proteins to the yeast vacuole. J. Cell Biol. *135*, 623–633.

Jakob, C.A., Burda, P., Roth, J., and Aebi, M. (1998). Degradation of misfolded endoplasmic reticulum glycoproteins in *Saccharomyces cerevisiae* is determined by a specific oligosaccharide structure. J. Cell Biol. *142*, 1223–1233.

Kagiwada, S., Hosaka, K., Murata, M., Nikawa, J., and Takatsuki, A. (1998). The Saccharomyces cerevisiae SCS2 gene product, a homolog of a synaptobrevin-associated protein, is an integral membrane protein of the endoplasmic reticulum and is required for inositol metabolism. J. Bacteriol. *180*, 1700–1708.

Knop, M., Finger, A., Braun, T., Hellmuth, K., and Wolf, D.H. (1996). Der1, a novel protein specifically required for endoplasmic reticulum degradation in yeast. EMBO J. *15*, 753–763.

Longtine, M.S., McKenzie, A., Demarini, D.J., Shah, N.G., Wach, A., Brachat, A., Philippsen, P., and Pringle, J.R. (1998). Additional modules for versatile and economical PCR-based gene deletion and modification in *Saccharomyces cerevisiae*. Yeast *14*, 953–961.

McCracken, A.A., and Brodsky, J.L. (1996). Assembly of ER-associated protein degradation in vitro: dependence on cytosol, calnexin, and ATP. J. Cell Biol. *132*, 291–298.

Mori, K., Ma, W., Gething, M., and Sambrook, J. (1993). A transmembrane protein with a cdc2+/CDC28-related kinase activity is required for signaling from the ER to the nucleus. Cell *74*, 743–756.

Mori, K., Kawahara, T., Yoshida, H., Yanagi, H., and Yura, T. (1996). Signalling from endoplasmic reticulum to nucleus: transcription factor with a basic-leucine zipper motif is required for the unfolded protein-response pathway. Genes Cells *1*, 803–817.

Ng, F.W., Nguyen, M., Kwan, T., Branton, P.E., Nicholson, D.W., Cromlish, J.A., and Shore, G.C. (1997). p28 Bap31, a Bcl-2/Bcl-XL- and procaspase-8-associated protein in the endoplasmic reticulum. J. Cell Biol. *139*, 327–338.

Pilon, M., Schekman, R., and Römisch, K. (1997). Sec61p mediates export of a misfolded secretory protein from the endoplasmic reticulum to the cytosol for degradation. EMBO J. *16*, 4540–4548.

Plemper, R.K., Böhmler, S., Bordallo, J., Sommer, T., and Wolf, D.H. (1997). Mutant analysis links the translocon and BiP to retrograde protein transport for ER degradation. Nature *388*, 891–895.

Pollard, M.G., Travers, K.J., and Weissman, J.S. (1998). Ero1p: a novel and ubiquitous protein with an essential role in oxidative protein folding in the endoplasmic reticulum. Mol. Cell *1*, 171–182.

Qu, D., Teckman, J., Omura, S., and Perlmutter, D. (1996). Degradation of a mutant secretory protein, alpha1-antitrypsin Z, in the endoplasmic reticulum requires proteasome activity. J. Biol. Chem. *271*, 22791–22795.

Roberg, K.J., Crotwell, M., Espenshade, P., Gimeno, R., and Kaiser, C.A. (1999). LST1 is a SEC24 homologue used for selective export of the plasma membrane ATPase from the endoplasmic reticulum. J. Cell Biol. *145*, 673–688.

Schena, M., Picard, D., and Yamamoto, K.R. (1991). Vectors for constitutive and inducible gene expression in yeast. Methods Enzymol. *194*, 389–398.

Schmitt, M.E., Brown, T.A., and Trumpower, B.L. (1990). A rapid and simple method for preparation of RNA from Saccharomyces cerevisiae. Nucleic Acids Res. *18*, 3091–3092.

Shamu, C.E., and Walter, P. (1996). Oligomerization and phosphorylation of the Ire1p kinase during intracellular signaling from the endoplasmic reticulum to the nucleus. EMBO J. *15*, 3028–3039.

Sherman, F. (1991). Getting started with yeast. Methods Enzymol. *194*, 3–21.

Sidrauski, C., and Walter, P. (1997). The transmembrane kinase Ire1p is a site-specific endonuclease that initiates mRNA splicing in the unfolded protein response. Cell *90*, 1031–1039.

Sidrauski, C., Cox, J.S., and Walter, P. (1996). tRNA ligase is required for regulated mRNA splicing in the unfolded protein response. Cell *87*, 405–413.

Sikorski, R.S., and Hieter, P. (1991). A system of shuttle vectors and yeast host strains designed for efficient manipulation of DNA in *Saccharomyces cerevisiae*. Genetics *122*, 19–27.

Trilla, J.A., Durán, A., and Roncero, C. (1999). Chs7p, a new protein involved in the control of protein export from the endoplasmic reticulum that is specifically engaged in the regulation of chitin synthesis in Saccharomyces cerevisiae. J. Cell Biol. *145*, 1153–1163.

Ward, C.L., Omura, S., and Kopito, R.R. (1995). Degradation of CFTR by the ubiquitin-proteasome pathway. Cell *83*, 121–127.

Werner, E.D., Brodsky, J.L., and McCracken, A.A. (1996). Proteasome-dependent endoplasmic reticulum-associated protein degradation: an unconventional route to a familiar fate. Proc. Natl. Acad. Sci. USA *93*, 13797–13801.

Wiertz, E.J., Tortorella, D., Bogyo, M., Yu, J., Mothes, W., Jones, T.R., Rapoport, T.A., and Ploegh, H.L. (1996). ER degradation of a misfolded luminal protein by the cytosolic ubiquitin-proteasome pathway. Nature *384*, 432–438.

Wodicka, L., Dong, H., Mittmann, M., Ho, M.H., and Lockhart, D.J. (1997). Genome-wide expression monitoring in *Saccharomyces cerevisiae*. Nat. Biotech. *15*, 1359–1367.

Zhou, M., and Schekman, R. (1999). The engagement of Sec61p in the ER dislocation process. Mol. Cell *4*, 925–934.